AAS 03-545

CONTROL OF NODE CROSSINGS IN SATURNIAN GRAVITY-ASSIST TOURS

Nathan Strange*
Jet Propulsion Laboratory / California Institute of Technology
4800 Oak Grove Drive, Pasadena, CA, 91109-8099

Abstract

In the Saturnian system, the control of the node-crossing point is important to avoid debris in Saturn's ring plane and to target flybys of moons other than Titan. This paper describes how to use gravity assists to control a spacecraft's node crossings.

INTRODUCTION

When Galileo first turned his telescope to Saturn in 1610, he noticed that it had strange 'handles'. Christiaan Huygens later explained that these mysterious handles were actually giant rings surrounding the planet. Saturn's ring system is the largest in the Solar System, with the main rings spanning a diameter of nearly 274,000 km.

Saturn has 30 named moons as of this writing. Saturn's largest moon, Titan, is larger than the planet Mercury and is the only moon in the Solar System to have a significant atmosphere. Titan's atmosphere is principly Nitrogen and 50% denser than Earth's. Saturn's other moons are much smaller than Titan, but fascinating nonetheless. Enceladus has the highest albedo of any object in the Solar system. Iapetus is a strange world of half snowy white terrain and half terrain as dark as lampblack. Table 1 shows the orbits of the major satellites[1] of Saturn, starting with Mimas which is just outside of the main rings.

Of Saturn's satellites, only Titan has strong enough gravity to be used for a gravity-assist tour. Tours of the Saturnian system, such as the Cassini tour,[2–4] are constructed from a sequence of Titan to Titan transfers. Flybys of Saturn's other moons may be accomplished by targeting a Titan to Titan transfer orbit to pass near a moon, but this is difficult. For example, the Cassini tour consists of 45 Titan flybys, but only 7 targeted flybys of Saturn's other moons.

Since most of Saturn's moons are in nearly equatorial orbits, it is easiest to find flybys of these moons with a spacecraft in a low inclination orbit. However, high inclination orbits are highly desirable to observe Saturn's rings, magnetosphere, and the high latitudes of the planet's atmosphere.

Saturn's rings make it difficult for a spacecraft to get close to the planet, as the ring debris may destroy a spacecraft that passes directly through the rings. In high inclination

*Member Engineering Staff, Navigation and Mission Design Section

Table 1: Saturn's Major Satellites

	Semi-Major Axis [R_S]	Period [days]	Eccentricity	Inclination (Saturn eq.)	GM (μ_{ga}) [km^3/s^2]	Radius [km]
Mimas	3.08	0.94	0.0206	0.01°	2.5	199
Enceladus	3.95	1.37	0.0001	0.01°	5.6	249
Tethys	4.88	1.89	0.0001	1.09°	44.1	523
Dione	6.26	2.74	0.0002	0.02°	77.3	560
Rhea	8.74	4.52	0.0009	0.00°	173.4	764
Titan	20.25	15.9	0.0288	0.36°	8978.1	2575
Hyperion	24.55	21.3	0.0175	1.01°	1.0	142
Iapetus	59.03	79.3	0.0284	15.42°	116.9	718
Phoebe	214.7	550.3	0.1644	152.0°	0.9	110

orbits, it is possible to have a periapsis closer to Saturn than the outer edge of the rings, as long as an orbit's node crossing does not pass through a ring. Cassini passes through a gap between the F and G rings upon arrival at Saturn and achieves a periapsis of only 1.3 R_S (Saturn Radii) for its orbit insertion.[2–4]

Much work has been done at JPL to study high inclination tours for the Cassini mission.[2–7] This paper extends this work to develop new analytic methods for targeting a spacecraft's node crossing point with Titan gravity assists. These techniques will enable Saturn tour designers to more easily avoid ring debris and find flybys of Saturn's other moons.

Future Saturn tour designs, such as the Cassini extended mission, will benefit from these techniques. However, the derivation of these techniques is general and may be applied to other high-inclination tour designs at Jupiter, Uranus, and Neptune.

ANALYSIS

We will assume that the spacecraft is in a simple two-body conic orbit around the central body (e.g. Saturn) except when it is in the immediate vicinity of the gravity-assist body. At that time, we will treat the spacecraft as being in a two-body conic orbit around the gravity-assist body (e.g. Titan). Such an approach is referred to as the method of *Patched Conics*.[8,9] From these assumptions, the conic equation gives the position of the spacecraft relative to the central body in the spacecraft's orbit plane. (Refer to the *Notation* section for an explanation of the symbols and subscripts used in this and subsequent equations.)

$$r_{sc} = \frac{a_{sc}(1 - e_{sc}^2)}{1 + e_{sc}\cos(f_{sc})} \tag{1}$$

The line of nodes of an orbit, illustrated in Fig. 1, is the line where the orbit plane intersects a reference plane, usually the central body's equatorial plane. The point where the orbit crosses from the southern hemisphere to the northern hemisphere is the *ascending node*, and the point where the orbit crosses from north to south is the *descending node*. The argument of periapsis (ω_{sc}) is defined as the angle from the ascending node crossing to the

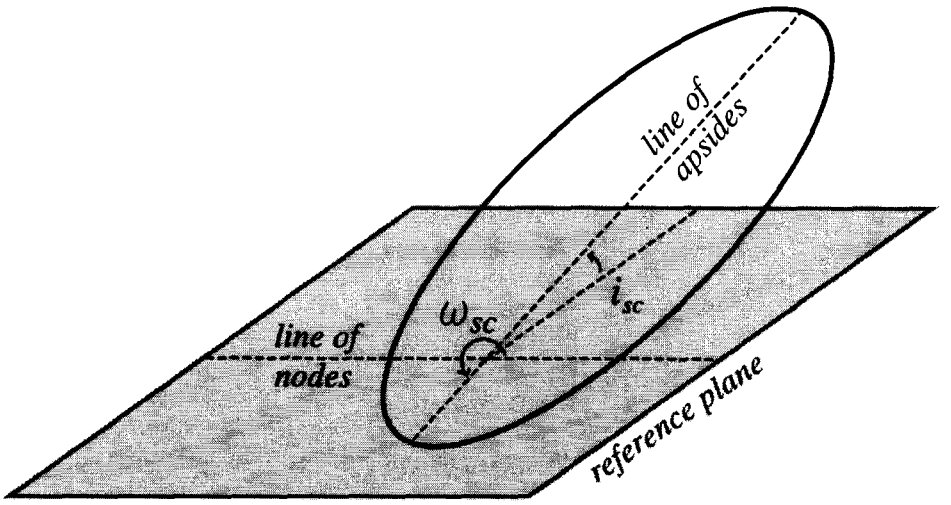

Figure 1: The Line of Nodes

periapsis of an orbit (see Fig. 1). Since true anomaly (f_{sc}) is measured from periapsis, the true anomaly of the ascending node crossing is $-\omega_{sc}$ and the true anomaly of the descending node is $\pi - \omega_{sc}$. Therefore, the radius of the ascending node (r_{asc}) and the radius of the descending node (r_{dsc}) are given by:

$$r_{asc} = \frac{a_{sc}(1-e_{sc}^2)}{1+e_{sc}\cos(-\omega_{sc})} = \frac{a_{sc}(1-e_{sc}^2)}{1+e_{sc}\cos(\omega_{sc})} \tag{2}$$

$$r_{dsc} = \frac{a_{sc}(1-e_{sc}^2)}{1+e_{sc}\cos(\pi-\omega_{sc})} = \frac{a_{sc}(1-e_{sc}^2)}{1-e_{sc}\cos(\omega_{sc})} \tag{3}$$

Equation 2 and Eqn. 3 may each be solved for the argument of periapsis, yielding the following two equations:

$$\cos(\omega_{sc}) = \frac{1}{e_{sc}}\left[\frac{a_{sc}}{r_{asc}}(1-e_{sc}^2)-1\right] \tag{4}$$

$$\cos(\omega_{sc}) = -\frac{1}{e_{sc}}\left[\frac{a_{sc}}{r_{dsc}}(1-e_{sc}^2)-1\right] \tag{5}$$

We may now write expressions for the radius of each node crossing in terms of the radius of the other node crossing:

$$r_{asc} = \frac{a_{sc}(1-e_{sc}^2)}{2-\frac{a_{sc}}{r_{dsc}}(1-e_{sc}^2)} \tag{6}$$

$$r_{dsc} = \frac{a_{sc}(1-e_{sc}^2)}{2-\frac{a_{sc}}{r_{asc}}(1-e_{sc}^2)} \tag{7}$$

Rather than use the planet's equator as the reference plane for defining node crossings, from now on we will use the orbit plane of the gravity-assist body, Titan. With this choice we ensure that Titan encounters in an inclined orbit must occur at a node crossing.[a] The

[a]If the spacecraft's orbit is not inclined, the longitude of the ascending node is arbitrary and may be chosen so that an encounter occurs at a node crossing.

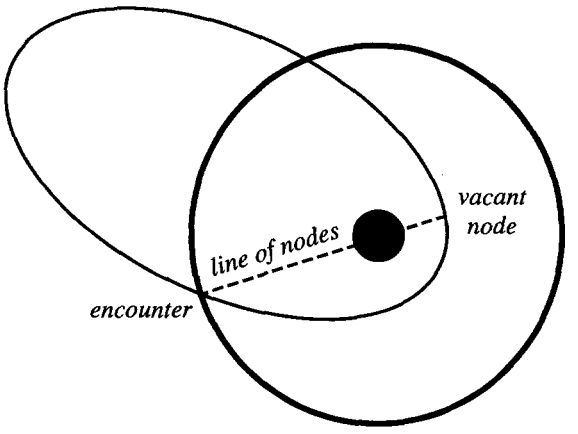

Figure 2: Illustration of the Vacant Node

node crossing point without a Titan encounter will be referred to as the *vacant node* as shown in Fig. 2. Titan's orbit plane is very close to the ring plane as well as the orbit planes of the inner satellites, and by tracking the radius of the vacant node crossing we can see if the spacecraft passes through a ring or if it passes near the orbit of another satellite.

We know the radius of the encounter (r_{enc}), which will occur at either the ascending node or the descending node. If we substitute (r_{enc}) into either Eqn. 6 or Eqn. 7, we arrive at the same expression, Eqn. 8, for the radius of the vacant node (r_{vac}). This allows us to compute the location of the vacant node crossing[b] without worrying about whether the gravity-assist encounter is at the ascending or the descending node.

$$r_{vac} = \frac{a_{sc}(1 - e_{sc}^2)}{2 - \frac{a_{sc}}{r_{enc}}(1 - e_{sc}^2)} \tag{8}$$

For an inclined spacecraft orbit, the encounter will always occur on the line of nodes. An encounter will usually occur at the same place in the gravity-assist body's orbit (as in Figure 2). In this case, the spacecraft's orbit will be resonant with the gravity-assist body's orbit and the time of flight between encounters will be some integer multiple of the gravity-assist body's period (i.e., a transfer with m spacecraft orbits during n gravity-assist body orbits will have a period of: $T_{sc} = (n/m)T_{ga}$). The other case of an inclined transfer is that of a backflip orbit[10] (also called a pi-transfer[2,3,11]) where an encounter occurs at both node crossings. Such transfers are difficult to achieve, and will not be discussed in this paper, but analytic expressions for these transfers are available.[11]

For a given transfer we will know the spacecraft orbit period, and may solve for the semi-major axis (a_{sc}) in Eqn. 8 with Kepler's Third Law:

$$a_{sc}^3 = \mu_{cb}\left(\frac{T_{sc}}{2\pi}\right)^2 \tag{9}$$

However, for the eccentricity (e_{sc}) in Eqn. 8 we need to look at the encounter with the gravity-assist body in more detail.

[b]Hyperbolic orbits may have only one node crossing. In such cases the vacant node does not exist and r_{vac} will be negative in Eqn. 8.

With the patched conic assumption, the spacecraft orbit during the flyby will be a hyperbola around the gravity-assist body. The velocity of the spacecraft on the hyperbola's asymptotes, the $\vec{v}_\infty$, is simply the velocity of the spacecraft (from its orbit around the central body) relative to the gravity-assist body:

$$\vec{v}_\infty = \vec{v}_{sc} - \vec{v}_{ga} \tag{10}$$

If we know the $\vec{v_\infty}$ vector after a flyby we can solve for the spacecraft velocity vector ($\vec{v}_{sc}$) and hence the orbit after the flyby. Conversely, we may also solve for the orbit before the flyby with the approach $\vec{v_\infty}$. Each $\vec{v_\infty}$ when combined with the location of the encounter with the gravity-assist body fully determines the spacecraft orbit around the central body.

To see how the $\vec{v_\infty}$ relates to the orbit around the central body, we construct an inertial reference frame using the instantaneous spacecraft postition and velocity relative to the central body at the encounter:

$$\hat{s}_1 = \frac{\vec{r}_{sc}}{r_{sc}} \tag{11}$$

$$\hat{s}_3 = \frac{\vec{r}_{sc} \times \vec{v}_{sc}}{r_{sc} v_{sc}} \tag{12}$$

$$\hat{s}_2 = \hat{s}_3 \times \hat{s}_1 \tag{13}$$

We may now write the spacecraft velocity as:

$$\vec{v}_{sc} = v_{sc}[\sin(\gamma_{sc})\hat{s}_1 + \cos(\gamma_{sc})\hat{s}_2] \tag{14}$$

With i_{sc} as the inclination of the spacecraft orbit relative to the plane of the gravity-assist body's orbit, we may write $\vec{v_{ga}}$ as follows:

$$\vec{v}_{ga} = v_{ga}[\sin(\gamma_{ga})\hat{s}_1 + \cos(\gamma_{ga})\cos(i_{sc})\hat{s}_2 - \cos(\gamma_{ga})\sin(i_{sc})\hat{s}_3] \tag{15}$$

From Eqn. 10, the $\vec{v_\infty}$ may be written as:

$$\vec{v}_\infty = [v_{sc}\sin(\gamma_{sc}) - v_{ga}\sin(\gamma_{ga})]\hat{s}_1 + [v_{sc}\cos(\gamma_{sc}) - v_{ga}\cos(\gamma_{ga})\cos(i_{sc})]\hat{s}_2 + v_{ga}\cos(\gamma_{ga})\sin(i_{sc})\hat{s}_3 \tag{16}$$

We may solve for the v_∞ magnitude by dotting the $\vec{v}_\infty$ vector with itself:

$$v_\infty^2 = v_{sc}^2 + v_{ga}^2 - 2v_{sc}v_{ga}[\sin(\gamma_{sc})\sin(\gamma_{ga}) + \cos(\gamma_{sc})\cos(\gamma_{ga})\cos(i_{sc})] \tag{17}$$

Next, the *vis viva* equation gives us a relation for the v_{sc} magnitude:

$$v_{sc}^2 = \mu_{cb}\left(\frac{2}{r_{enc}} - \frac{1}{a_{sc}}\right) \tag{18}$$

Notice that in Eqn. 18, the v_{sc} magnitude for a given orbit is a function of only r_{enc}. If the gravity-assist body is in a circular orbit, then v_{sc} will be the same for every flyby unless a maneuver or another flyby changes r_{enc} or a_{sc}.

Orbital angular momentum gives us a an expression for flight path angle (γ_{sc}) at the encounter:

$$h_{sc} = r_{enc}v_{sc}\cos(\gamma_{sc}) = \sqrt{\mu_{cb}a_{sc}(1 - e_{sc}^2)} \tag{19}$$

$$\cos(\gamma_{sc}) = \frac{1}{r_{enc}v_{sc}}\sqrt{\mu_{cb}a_{sc}(1 - e_{sc}^2)} \tag{20}$$

We see that like v_{sc}, $\cos(\gamma_{sc})$ at an encounter depends only on r_{enc} and parameters that are constant for a given orbit. Since i_{sc} won't change between flybys without a maneuver, by Eqn. 17, the v_∞ magnitude will also be constant if r_{enc} doesn't change. Since Titan's orbit is nearly circular (see Table 1), v_∞ magnitude will change little in ballistic Saturnian tours.

If we can solve Eqn. 17 for $\cos(\gamma_{sc})$ independent of $\sin(\gamma_{sc})$, we may use Eqn. 20 and Eqn. 17 to solve for e_{sc} as a function of the spacecraft's v_∞ magnitude, inclination, and semi-major axis. In order to solve for $\cos(\gamma_{sc})$ in Eqn. 17, we will assume that the gravity-assist body is in a circular orbit. This means that $\gamma_{ga} = 0$ and v_{ga} is given by:

$$v_{ga} = \sqrt{\frac{\mu_{cb}}{r_{enc}}} \tag{21}$$

Now we may combine Eqn. 18 with Eqn. 17:

$$v_\infty^2 = \mu_{cb}\left(\frac{3}{r_{enc}} - \frac{1}{a_{sc}} - 2\cos(\gamma_{sc})\cos(i_{sc})\sqrt{\frac{2}{r_{enc}^2} - \frac{1}{a_{sc}r_{enc}}}\right) \tag{22}$$

and solve for $\cos(\gamma_{sc})$:

$$\cos(\gamma_{sc}) = \frac{\frac{3}{r_{enc}} - \frac{1}{a_{sc}} - \frac{v_\infty^2}{\mu_{cb}}}{2\cos(i_{sc})\sqrt{\frac{2}{r_{enc}^2} - \frac{1}{a_{sc}r_{enc}}}} \tag{23}$$

We solve for e_{sc} from Eqn. 20 and Eqn. 23:

$$e_{sc}^2 = 1 - \frac{r_{enc}}{a_{sc}}\left(\frac{3 - \frac{r_{enc}}{a_{sc}} - \frac{v_\infty^2 r_{enc}}{\mu_{cb}}}{2\cos(i_{sc})}\right)^2 \tag{24}$$

In order to simplify, Eqn. 24, we introduce the following non-dimensional parameter[c] which depends only on v_∞ and a_{sc}:

$$p = \left(\frac{3 - \frac{r_{enc}}{a_{sc}} - \frac{v_\infty^2 r_{enc}}{\mu_{cb}}}{2\cos(i_{sc})}\right)^2 \tag{25}$$

This simplifies Eqn. 24 to:

$$e_{sc}^2 = 1 - p\frac{r_{enc}}{a_{sc}} \tag{26}$$

Finally, substituting Eqn. 26 into Eqn. 8 yields the following expression for the vacant node crossing radius:

$$\frac{r_{vac}}{r_{enc}} = \frac{p}{2-p} \tag{27}$$

Since Titan is in a nearly circular orbit, we will have the same v_∞ throughout a tour unless we perform a maneuver.[11] This then allows us to compute the vacant node radius as a function of inclination and period from Eqn. 25 and Eqn. 27.

[c]This non-dimensional parameter is actually the semi latus rectum divided by r_{enc}.

Allowable Range for p

Before using Eqn. 27 or Eqn. 26, we need to be aware of constraints on apoapsis and periapsis of the spacecraft's orbit. The spacecraft's apoapsis must be greater than or equal to r_{enc} and the periapsis must be less than or equal to r_{enc}:

$$a_{sc}(1 - e_{sc}) \leq r_{enc} \leq a_{sc}(1 + e_{sc}) \tag{28}$$

Using Eqn. 26, we may rewrite the above inequality as:

$$\frac{p}{1 + e_{sc}} \leq 1 \leq \frac{p}{1 - e_{sc}} \tag{29}$$

The right side of this inequality yields:

$$e_{sc} \geq 1 - p \tag{30}$$

and the left side yields:

$$e_{sc} \geq p - 1 \tag{31}$$

We may square Eqn. 30 to get a constraint valid when $p \leq 1$ and squaring Eqn. 31 yields a constraint valid for $p \geq 1$. Both actions yield the same inequality:

$$p^2 - 2p + 1 \leq e_{sc}^2 \tag{32}$$

Using Eqn. 26, this simplifies to:

$$p(2 - p) \geq p\frac{r_{enc}}{a_{sc}} \tag{33}$$

The definition of p in Eqn. 25 insures that p will always be positive. Therefore, we may divide p from both sides of Eqn. 33 and arrive at the constraint below:

$$0 \leq p \leq 2 - \frac{r_{enc}}{a_{sc}} \tag{34}$$

In the case of a hyperbolic orbit, there may not always be a vacant node crossing. Requiring r_{vac} in Eqn. 27 to be positive, we arrive at the following constraint on p for a hyperbolic orbit which is more restictive than Eqn. 34:

$$0 \leq p \leq 2 \tag{35}$$

RESULTS

Constrained by Eqn. 34 or Eqn. 35, we may now use Eqn. 27 to design node crossings in a gravity-assist tour. All that's left to do is to check the vacant node crossing for ring debris or an encounter with one of Saturn's other moons.

Table 2: Saturn's Ring System

Ring or Region	Inner Radius (r_{in})		Outer Radius (r_{out})		Half Thickness (t_{ring})
	[km]	[R_S]	[km]	[R_S]	[km]
D Ring	66970	1.11	74470	1.23	1
C Ring	74500	1.23	92000	1.52	1
B Ring	92000	1.52	117400	1.95	1
Cassini Division	117400	1.95	122170	2.03	–
A Ring	122170	2.03	136780	2.27	2
F Ring	140180	2.32	140260	2.32	50
Jan/Ep Debris	149600	2.48	153300	2.54	900
G Ring	165000	2.73	176000	2.92	720
Mimas Debris	181170	3.00	189870	3.15	4800
E Ring	180000	2.98	300000	4.97	10000

Rings

Table 2 shows the Saturn ring system.[12–14] Included are possible debris regions near the orbits of Mimas and the co-orbital moons, Janus and Epimetheus. The existence of such debris fields is uncertain, but these regions should be avoided until the nature of any debris is better known. The E Ring is included in Table 2, but is thought to be very low density and the Cassini spacecraft will frequently pass through the E Ring, taking precautions to protect delicate parts of the spacecraft from dust impacts.[14] Although the Cassini Division appears to be a gap in the rings, there is evidence of material in this region[12] and it may be risky to plan a pass through this region. In general, the extent of Saturn's ring system and debris fields is still not well known, and the regions in Table 2 will be much better known after the Cassini mission.

While we don't want one of the spacecraft's node crossings to be in the middle of a ring, we also don't want an orbit to pass through a ring before or after a node crossing. To avoid the ring debris, we will draw a rectangular torus around a ring, as in Fig. 3, and avoid that torus. The simple geometry of the torus is much easier to work with than the complex and often poorly understood particle distributions in a ring or debris field. We can guarantee that we will avoid the ring debris if we do not pass through the torus around the ring, so from now on we will treat the rings as if they are simply rectangular tori.

Figure 3 shows orbits whose node crossings are outside of a ring yet still pass through the ring. To account for such grazing orbits we may treat a ring's inner (x_{in}) and outer (x_{out}) boundaries as functions of inclination (where r_{in}, r_{out}, and t_{ring} are given in Table 2):

$$x_{in} = r_{in} - \frac{t_{ring}}{\tan(i_{sc})} \tag{36}$$

$$x_{out} = r_{out} + \frac{t_{ring}}{\tan(i_{sc})} \tag{37}$$

If a spacecraft's node crossing is between x_{in} and r_{out} then it will pass through the ring. But if the node crossing is between r_{out} and x_{out}, it will only pass through a ring if the spacecraft's periapsis distance is less than r_{out}.

Figure 4 is a plot of vacant node radius vs. inclination showing the regions where orbits pass through the rings. The darkly shaded regions for each ring show where a spacecraft will always pass through a ring ($x_{in} \leq r_{vac} \leq r_{out}$), and the lightly shaded regions are where a spacecraft will pass through a ring if the periapsis is less than r_{out} ($r_{out} < r_{vac} \leq x_{out}$). Also plotted are dashed lines showing the vacant node crossings for orbits as a function of inclination. Each orbit has $v_\infty = 5.95$ km/s and $r_{enc} = 19.68$ R_S which corresponds to Cassini at the end of its primary mission. Each dashed line is a plot of Eqn. 27 and is labeled with the period of the orbits on that line as a resonance of *Titan revs : spacecraft revs.*

Using Eqn. 27, Eqn. 36, and Eqn. 37, similar plots can be generated for other values of v_∞ and r_{enc}. For a given Saturnian tour, Titan v_∞ and r_{enc} are roughly constant, and one plot could be used for an entire tour.[d]

Satellite Encounters

Gravity-assist tours at Saturn have only one gravity-assist body available, Titan. All of Saturn's other moons are not massive enough to provide a useful gravity-assist. Flybys of Saturn's other moons may be designed by finding Titan to Titan transfers which happen to pass close to a moon.[7] Finding satellite encounters can be especially difficult when a spacecraft is in an inclined orbit, as the spacecraft must cross the radius of a moon's orbit in that moon's orbit plane.

If all of Saturn's moons were in circular coplanar orbits, to see if we cross a satellite's orbit we would simply check if an orbit's vacant node crossing was equal to the radius of a satellite's orbit. Such an assumption may work for Saturn's inner moons, but does not hold for the outer satellites that have significant eccentricity and inclination.

Another approach is to construct a ring out of all possible points a satellite's orbit may enter. Such an *encounter box* can be constructed by treating a satellite's periapsis like a ring's inner radius and a satellite's apoapsis as a rings outer radius. Equation 38 gives an expression for the half thickness[e] of an encounter box:

$$t_{sat} = a_{sat}(1 + e_{sat})\sin(i_{sat}) \tag{38}$$

Table 3 gives the encounter boxes for the satellites along with their inclination relative to Titan's orbit (Table 1 gives inclination relative to Saturn's equator). A spacecraft's orbit passing through an encounter box is a necessary condition for a satellite encounter, but not a sufficient condition. In addition, the spacecraft must cross the satellite's orbit and do so when the satellite is in that position in its orbit. However, encounter boxes are still useful in that we are able to exclude many orbits that do not pass through an encounter box.

[d]Because of Titan's eccentricity, v_∞ and r_{enc} do vary by a small amount. However, these quantities vary mostly with non-resonant Titan transfers and once a spacecraft is in a sequence of high-inclination resonant transfers v_∞ and r_{enc} will vary only due to maneuvers. At the end of the Cassini mission, Cassini is in a very high inclination (about 75°) and as such, Fig. 4 could be used to design the Cassini extended mission and would only possibly need to be updated after Cassini achieved a low inclination and performed non-resonant Titan to Titan transfers.

[e]Equation 38 uses the product of a satellite's apoapsis and its inclination. Apopsis rather than a radius 90°from a satellite's node crossing is used because a satellite's line of apides will precess and using the apoapsis in Eqn. 38 avoids having to account for this precession.

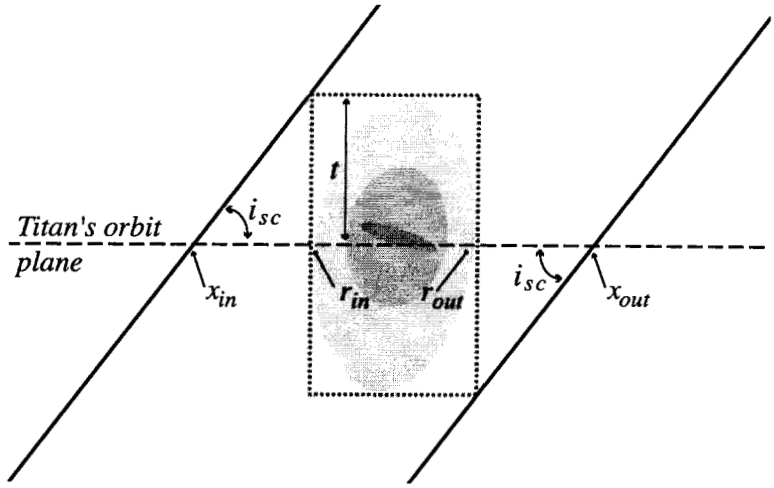

Figure 3: Orbits Grazing a Ring

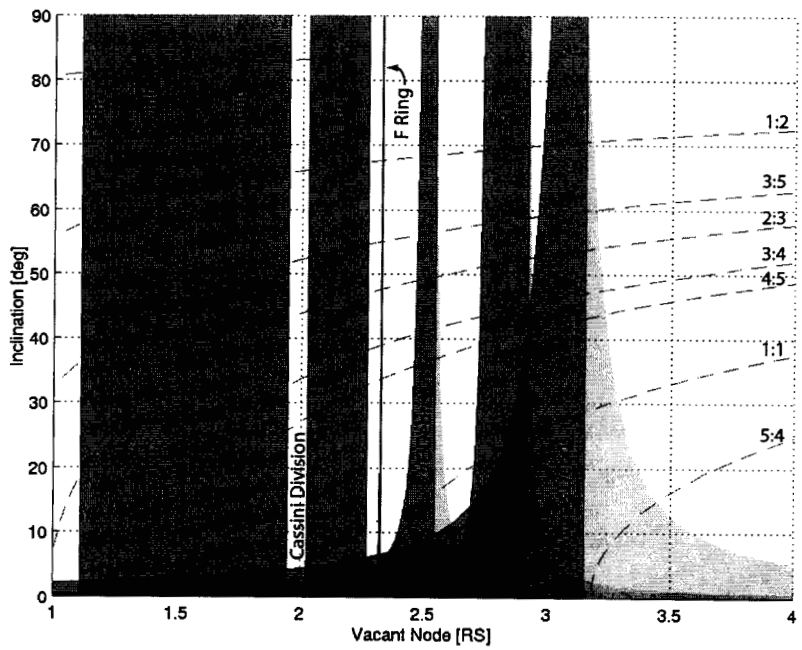

Figure 4: Node Crossings and Rings [$v_\infty = 5.95$ km/s, $r_{enc} = 19.68$ R_S]

Table 3: Encounter Boxes For Satellites

	$r_{in} = a_{sat}(1 - e_{sat})$ [R_S]	$r_{out} = a_{sat}(1 + e_{sat})$ [R_S]	i_{sat} (Titan orb.)	t_{sat} [R_S]
Mimas	3.01	3.14	1.48°	0.081
Enceladus	3.94	3.95	0.36°	0.025
Tethys	4.88	4.88	0.75°	0.064
Dione	6.25	6.26	0.34°	0.056
Rhea	8.73	8.74	0.54°	0.082
Titan	19.67	20.84	0.00°	0.000
Hyperion	24.12	24.98	0.67°	0.291
Iapetus	57.35	60.71	15.12°	15.838
Phoebe	179.39	249.98	151.67°	118.646

Equation 39 and Eqn. 40 give the inner and outer boundaries of an encounter box in a spacecraft's orbit plane:

$$x_{in} = a_{sat}\left(1 - e_{sat} - \frac{(1 + e_{sat})\cos(i_{sc})}{\tan(i_{sc})}\right) \tag{39}$$

$$x_{out} = a_{sat}\left(1 + e_{sat} + \frac{(1 + e_{sat})\cos(i_{sc})}{\tan(i_{sc})}\right) \tag{40}$$

Figure 5 shows the encounter boxes for the satellites inside of Titan's orbit. The darkly shaded regions show where a spacecraft will always pass through an encounter box ($x_{in} \leq r_{vac} \leq a_{sat}(1+e_{sat})$), and the lightly shaded regions are where a spacecraft will pass through a box if the periapsis is less than a satellite's apoapsis ($a_{sat}(1 + e_{sat}) < r_{vac} \leq x_{out}$). All of the orbits have $v_\infty = 5.95$ km/s and $r_{enc} = 19.68$ R_S and each dashed line is labeled with a resonance as in Fig. 4.

Figure 6 shows the encounter boxes of the satellites from Dione out. For the satellites outside of Titan's orbit, the spacecraft's apoapsis must be greater than a satellite's periapsiss to pass through an encounter box. The darkly shaded regions show where a spacecraft will always pass through an encounter box ($a_{sat}(1 - e_{sat}) \leq r_{vac} \leq x_{in}$), and the lightly shaded regions are where a spacecraft will pass through a box if the apoapsis is less than a satellite's periapsis ($x_{in} < r_{vac} \leq a_{sat}(1 - e_{sat})$). All of the orbits have $v_\infty = 5.95$ km/s and $r_{enc} = 19.68$ R_S and each dashed line is labeled with a resonance as in Fig. 4 and Fig. 5.

Phoebe and Iapetus have significant inclination relative to Titan's orbit, resulting in large encounter boxes. Phoebe's encounter box is not plotted on Fig. 6 because its encounter box is too large to really be useful. Even Iapetus's box is a very large region in which to look for an Iapteus encounter. In addition to having a node crossing inside of an encounter box, the spacecraft's line of nodes must have the proper orientation for the spacecraft's orbit to intersect the orbits of Iapetus and Phoebe, and this is not accounted for in this analysis.

Once v_∞ is known for a Saturn tour, plots such as Fig. 5 and Fig. 6 may be generated to identify orbits on which encounters with other satellites are possible. These orbits may then be compared to the satellite ephemeris to see if any satellite encounters do occur.

Figure 5 and Fig. 6 may be used to plan a sequence of Titan flybys to set up the proper spacecraft period and inclination to enter a satellite's encounter box. Satellite encounters

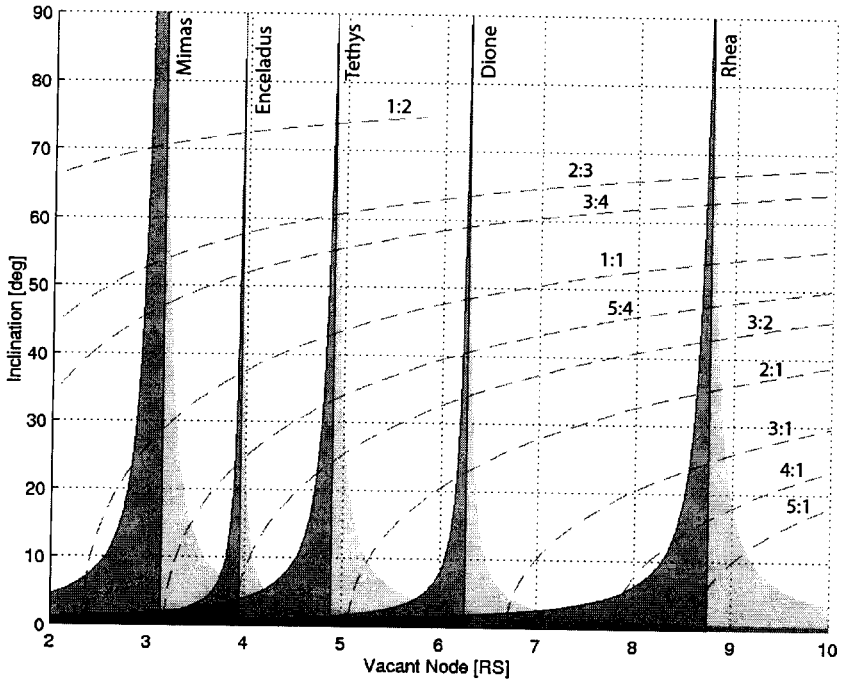

Figure 5: Node Crossings, Inner Satellites [$v_\infty = 5.95$ km/s, $r_{enc} = 19.68$ R_S]

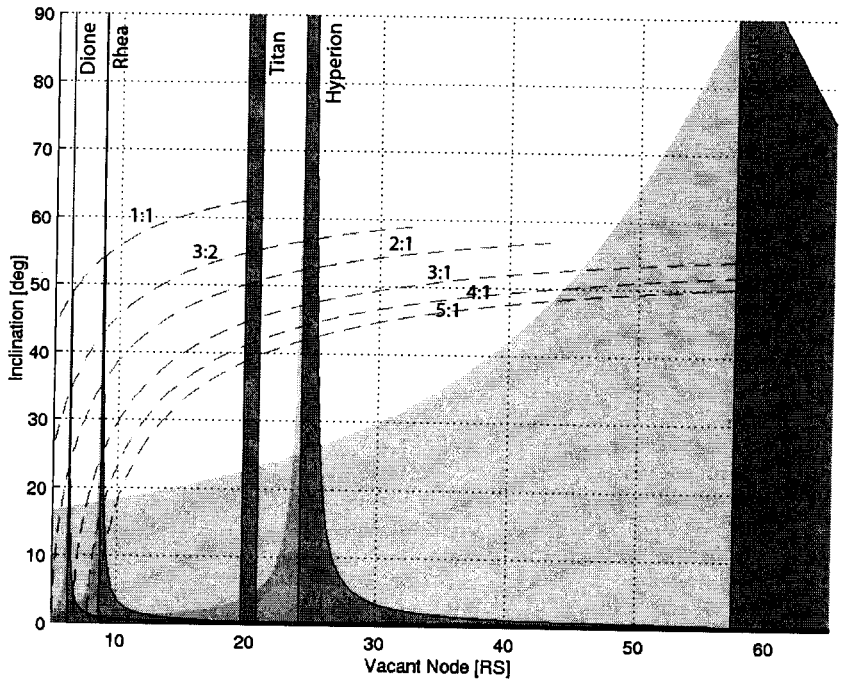

Figure 6: Node Crossings, Outer Satellites [$v_\infty = 5.95$ km/s, $r_{enc} = 19.68$ R_S]

are difficult to achieve in high inclination tours, and it is a great advantage to be able to plan a sequence of Titan flybys to set up geometry favorable for a satellite encounter. Without controlling the vacant node crossing, such encounters can only be found through a laborious trial and error process.[7]

Periapsis and Apoapsis

For the lightly shaded regions in Figures 4-6 we need to check the spacecraft's periapsis or apoapsis to find out if it passes through a ring or an encounter box. Since Eqn. 26 gives the eccentricity of the spacecraft's orbit, we may make plots of the spacecraft's periapsis or apoapsis similar to Figures 4-6.

Figure 7 shows the periapsis radius for different resonances and the outer radius of the encounter boxes of the inner satellites as well as r_{out} for the outer rings. Figure 7 allows us to check the lightly shaded areas in Fig. 4 and Fig. 5. It turns out that almost every orbit shown on Fig. 4 in a lightly shaded area passes through a ring, and almost every orbit on Fig. 5 in a lightly shaded area passes through an encounter box. Because x_{out} in Eqn. 37 and Eqn. 40 approaches infinity as inclination reaches zero, all vacant nodes will be in a lightly shaded region for every satellite and every ring as i_{sc} nears zero. Figure 7 is then useful to exclude orbits in low inclination cases.

Figure 8 shows the apoapsis of different resonances with the inner radius of the encounter boxes for the outer satellites to use with Fig. 6. Resonances of 3:1 and higher have apoapses above 65 R_S and are not shown on this plot. Figure 8 shows that orbits with resonances less than 2:1 on Fig. 6 in a lightly shaded area will not reach Iapetus.

CONCLUSION

Saturn's rings are both a target of high scientific interest and a hazard to the spacecraft. The methods developed in this paper for controlling the vacant node crossing allow the tour designer to get close to the ring system for science while avoiding known debris. Saturn's satellites are also targets of high scientific interest, but are difficult to reach, particularly in high inclination phases of the tour. This paper also developed methods for narrowing the search for these flybys. By excluding many Titan transfers, the tour designer may now focus the search for satellite flybys.

Tour design at Saturn is restricted by the fact that only Titan is available for meaningful gravity assists. However, this constraint also simplifies the tour design problem and allows many analytic techniques that would not be possible in a more complicated system. There is much more work to be done in developing an analytic theory of tour design, and it is hoped that this paper will stimulate interest in this area. It should be possible to predict orbits that will encounter other satellites based on the phase angle between Titan and that satellite. It is also important to calculate the flyby altitude and b-plane angle needed for a given period and inclination change. This would help to predict how many flybys are needed to get from a starting state to an orbit that encounters a satellite or has some other desired orbit geometry.

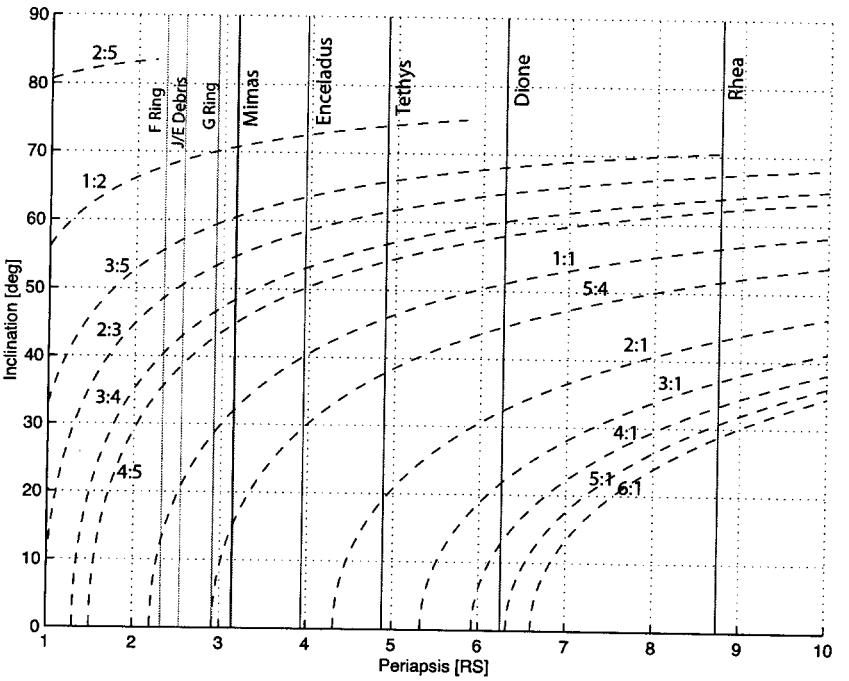

Figure 7: Periapsis vs. Inclination [$v_\infty = 5.95$ km/s, $r_{enc} = 19.68$ R_S]

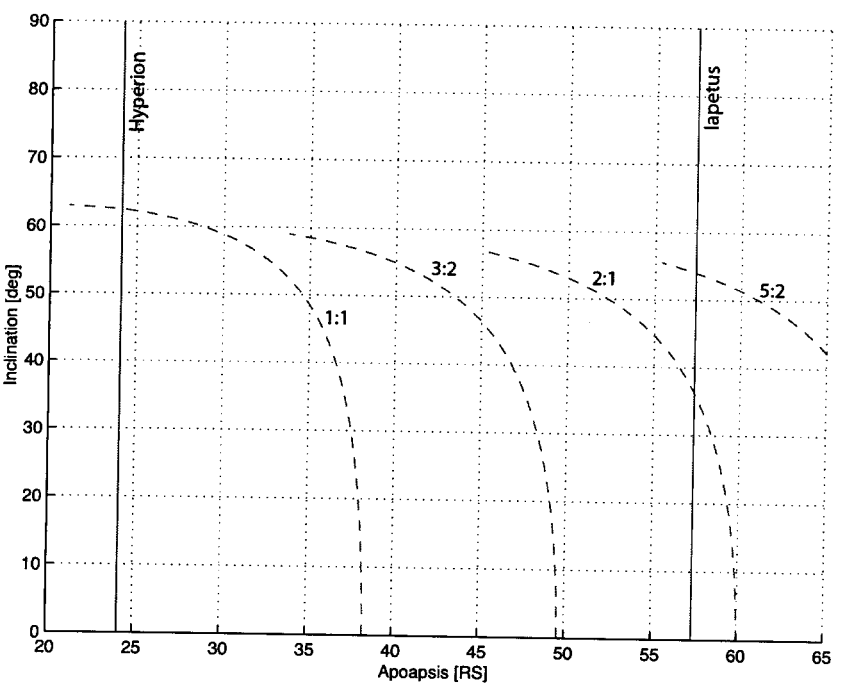

Figure 8: Apoapsis vs. Inclination [$v_\infty = 5.95$ km/s, $r_{enc} = 19.68$ R_S]

ACKNOWLEDGMENTS

The research described in this paper was carried out at the Jet Propulsion Laboratory, California Institute of Technology, under contract with the National Aeronautics and Space Administration. I would like to thank John Smith and Aron Wolf for teaching me the methods used for Cassini's high inclination tour design, and I would like to thank Dave Seal for his help in understanding the debris regions at Saturn. I would also like to thank Jon Sims and Gene Bonfiglio for reviewing this paper and for their helpful suggestions.

NOTATION

Symbols

γ	flight path angle relative to central body
ΔV	change in velocity magnitude
μ	gravitational parameter (GM)
ω	argument of periapsis relative to central body
a	semi-major axis relative to central body
e	eccentricity relative to central body
f	true anomaly relative to central body
h	specific orbital angular momentum
i	inclination relative to the gravity-assist body's orbit
p	non-dimensional orbit parameter defined in Eqn. 25
$\vec{r}$	displacement from the central body
r	magnitude of $\vec{r}$
r_{asc}	radius of ascending node
r_{dsc}	radius of descending node
r_{enc}	distance of encounter from central body
r_{in}	ring inner radius
r_{out}	ring outer radius
R_S	units of Saturn radii (1 R_S= 60330 km)
r_{vac}	distance of vacant node from central body
$\hat{s}_1, \hat{s}_2, \hat{s}_3$	a vector basis tied to the spacecraft's orbit
T	orbit period
t_{ring}	ring half thickness
t_{sat}	encounter box half thickness
$\vec{v}$	velocity vector relative to central body
v	magnitude of $\vec{v}$
$\vec{v_\infty}$	v-infinity vector relative to gravity-assist body
v_∞	magnitude of $\vec{v_\infty}$

Subscripts

cb	quantity is for central body
ga	quantity is for the gravity-assist body
sat	quantity is for a natural satellite
sc	quantity is for the spacecraft

REFERENCES

[1] "Planetary Satellite Mean Orbital Parameters," *http://ssd.jpl.nasa.gov/sat_elem.html*, Jet Propulsion Laboratory, Pasadena, CA.

[2] Smith, J.C., "Description of Three Candidate Cassini Satellite Tours," AAS/AIAA Space Flight Mechanics Meeting, AAS Paper 98-106, Monterey, California, Feb. 1998.

[3] Wolf, A.A., "Touring the Saturnian System," *Space Science Reviews*, Vol. 104, 2002, pp. 101-128.

[4] Strange, N.J., Goodson, T.D., and Hahn, Y., "Cassini Tour Redesign for the Huygens Mission," AIAA/AAS Astrodynamics Conference, AIAA Paper 2002-4720, Monterey, California, Aug. 2002.

[5] Wolf, A.A., "High Inclination Orbit Sequences for the Cassini Tour," JPL IOM 312/96.4-0002, Jan. 1996. (*JPL internal IOM*)

[6] Wolf, A.A., "Maximizing Inclination in Cassini Tours," JPL IOM 312/94.4-2058, Sep. 1994. (*JPL internal IOM*)

[7] Wolf, A.A., Smith, J.C., Knocke, P.C., and Garner, G.J., "Icy Satellite Flybys in Cassini Tours," JPL IOM 312/95.4-2084, Apr. 1995. (*JPL internal IOM*)

[8] Broucke, R.A., "The Celestial Mechanics of Gravity Assist," AIAA/AAS Astrodynamics Conference, AIAA Paper 88-4220, Minneapolis, Minnesota, Aug. 1988.

[9] Cesarone, R.J., "A Gravity Assist Primer," *AIAA Student Journal*, Vol. 16, Spring 1989, pp. 16-22.

[10] Uphoff, C., "Orbit Design Concepts for Jupiter Orbiter Missions," AIAA Mechanics and Control Conference, AIAA Paper 74-781, Anaheim, California, Aug. 1974.

[11] Strange, N.J. and Sims, J.A., "Methods for the Design of V-Infinity Leveraging Maneuvers," AAS/AIAA Astrodynamics Conference, AAS Paper 01-473, Québec, Québec, July/Aug. 2001.

[12] Cuzzi, J. N., Lissauer, J.J., Esposito, L.W., Holberg, J.B., Marouf, E.A., Tyler, G.L., and Boischot, A., "Saturn's Rings: Properties and Processes," *Planetary Rings*, University of Arizona Press, Tucson, Arizona, 1984. pp. 73-199.

[13] Cuzzi, J.N., Colwell, J.E., Esposito, L.W., Porco, C.C., Murray, C.D., Nicholson, P.D., Spilker, L.J., Marouf, E.A., French, R.C., Rappaport, N., and Muhleman, D., "Saturn's Rings: Pre-Cassini Status and Mission Goals," *Space Science Reviews*, Vol. 104, 2002, pp. 209-151.

[14] Seal, D.A., "Cassini Dust Protection Plan," JPL IOM: D-2425, *to be published this fall.* (*JPL internal IOM*)